



Rain Attenuation and Parameterization of Rainfall Microstructure using a Vertically Pointing Micro Rain Radar in Tropical Regions

Tomwa, Akinyemi C.

Department of Physics and Electronics, Adekunle Ajasin University, Akungba-Akoko, OndoState, Nigeria. E-mail: akinyemi.tomiwa@aau.edu.ng or tomiwaakinyemiclem@gmail.com

Article Info

Keywords: Drop size distribution, stratiform, convective, radar reflectivity, and rain rates

Received 8 October 2023

Revised 28 November 2023

Accepted 29 November 2023

Available online 21 Jan 2024

<https://doi.org/10.5281/zenodo.10543634>
ISSN-2682-5821/© 2023 NIPES Pub. All rights reserved.

Abstract

At Akure (Lat 5° 15'E, Long 7° 15'N) in South-Western Nigeria, Micro Rain Radar was used to measure the vertical profiles of rainfall characteristics including drop size distribution, rain rate, liquid water content, fall velocity, and radar reflectivity during the rainy periods of August and September 2014. These parameters' vertical distributions at various heights and the predicted attenuation were shown for the range of 0 to 4800 m. 30 range gates with a 160 m height step are used for the measurement. We assessed how drop size distribution, rain rate, and liquid water content varied with height. The results obtained show a good correlation between the measured parameters, demonstrating that specific liquid water content increases with increasing rain rate for both stratiform and convective rain types in this region of the world. Estimation of the Liquid Water Content (LWC) with heights reveals that stratiform rain for all the estimated heights contributes more to the rain event. The predicted rain attenuation time series which is also a function of rain rate (RR) varies in a similar pattern and its effect is higher at the ground level than at high altitudes.

1.0. Introduction

Water is crucial for understanding dynamic atmospheric processes, weather forecasting, and climate research since it plays a significant role in the atmosphere. Communication fundamentals include accurate measurement and forecasting of rainfall's spatial and temporal distribution. Numerous researchers have measured a variety of rainfall properties using a variety of tools, including the rain gauge and the disdrometer. There are challenges in characterizing the size spectra of raindrops since they are frequently large enough to have a size-dependent shape that cannot be described by a single length. The equivalent drop diameter D_0 , which is the diameter of a sphere with exactly the same volume as the deformed drop, is the traditional method for describing rain spectra [1].

In order to estimate dropsizes from area detectors, interpret Doppler radar data, and simulate rain, it is crucial to understand the actual raindrop fall speeds. In research areas like hydrology and soil erosion, the speed at which raindrops fall is also helpful. Several researchers have evaluated the final velocity of drops under laboratory circumstances at sea level. Raindrop fall velocity is also an important quantity and related to the measurements of Raindrop size

distributions (RSDs) and various integral quantities like rain rate [2]. In earlier research, it was considered that a raindrop's fall speed $v_s(D)$ is mostly influenced by its size and is equivalent to that of water drops falling in still air. The equilibrium of two opposing gravitational and drag forces acting on the drop during its vertical journey yields the raindrop terminal velocity, or v_t . A falling drop can come into contact with other cloud and precipitation particles at the time the formation and development of rain, but gravitational effects are dominant in clouds due to the larger terminal velocities of large raindrops, which cause them to catch up with and clash with smaller drops in their paths as they fall [3]. The results of raindrop collision incidents could result in bouncing, clumping, or breakup, and understanding of the chances of occurrence of each of these three outcomes can help in predicting the evolution of drop size distributions. Raindrops' fall speeds have been measured by numerous investigations using a variety of sensors close to the ground, and it has been shown that these measurements occasionally diverge from those made by [4], which are typically considered as a benchmark for $v_t(D)$. Modest raindrop fall speed deviations from $v_t(D)$ and cited drop breakup as a very plausible explanation for their findings, but they did not rule out alternative possibilities such turbulence brought on by air motions [5]. Each aqueous particle develops into a minuscule droplet with a diameter of 0.0001 to 0.005 centimetres. The size of the droplets varies because to the size variation of the particles. But after the developing droplet grows to a diameter of 0.5 mm or greater, we can refer to it as a raindrop [6].

1.1. The Micro Rain Radar (MRR)

The micro rain radar is a Doppler radar that utilizes the Doppler Effect to generate velocity information about distant objects. This is accomplished by sending a microwave signal in the direction of the intended target, listening for its reflection, and determining how the motion of the target has affected the frequency of the returned signal.

The importance of rain drop size distribution (DSD) has grown along with the prominence of rainfall measurements. Radio waves are emitted by the transmitter, reflected by the targets, and picked up by a receiver. Radio waves are easily amplified since the returning radio signals are often weak. As a result, radar has the ability to identify objects at distances where other emissions like sound or visible light would be too feeble to do so [7].

The Micro Rain Radar (MRR) is a vertically oriented frequency modulated continuous wave Doppler radar that emits electromagnetic waves (EM) solely in one direction. The MRR is a frequency modulated continuous-wave radar, which means that it constantly transmits EM waves while the frequency fluctuates (modulates). A wavelength of approximately 1.24 cm corresponds to an average frequency of 24 GHz. Raindrops, hail, and snowflakes are the principal components of the atmosphere that have an impact on the transmitted EM waves. The portion of the EM waves that are reflected back towards the ground and can be picked up by the MRR receiver. According to [7], the reflected signal provides information regarding the quantity, speed, and size of the drops in the atmosphere. We may utilize the Doppler Effect to calculate the fall speed along with factors such as the droplet size distribution, the rain rate, the liquid water content, and the accompanying fall velocity when the drops are falling along the path to the ground. When the rain radar hits the obstruction, it reflects EM waves traveling through the atmosphere at the speed of light at time T in seconds. As a result, the receiver receives the reflection of droplets that are close to the MRR before the droplets themselves. With a height resolution of 160 m and this propagation time, we can discern between 30 height levels. The Federal University of Technology Akure, Nigeria, is home to the Micro Rain Radar that was utilised for this project. To a great extent, super high frequency (SHF) and extremely high frequency (EHF) bands is currently being explored for satellite capabilities as the need

for communication solutions grow daily. The necessity to satisfy the requirement for larger data rates for various communication and multimedia need is caused by the daily increase in allocation towards the higher end of the electromagnetic spectrum, particularly over 10 GHz. It is crucial to remember that rain, which can attenuate sound by several decibels, has been found to be a significant cause of visual deterioration at millimetre wave frequencies (above 10 GHz) and to be an impediment in terrestrial link design, particularly for tropical and equatorial regions that receive heavy precipitation [8, 9].

1.2. Drop Size Distribution

The relationship between terminal fall velocity (v) and drop diameter (D), discovered empirically by [4], and analytically developed by [10], is used to derive drop size ranges. Using a generalized version with an adjustment for height-dependent density for the fall velocity $d_v(h)$

$$N(D) = \frac{\eta(D)}{\sigma(D)} \quad (1)$$

where D = the drop diameter
 $\sigma(D)$ = the back scattering cross section

1.3. Rain Rate

The differential rain rate $\{rr(D)\}$ is equal to the volume of the differential droplet number density $(\frac{\pi}{6}) \times N(D)D^3$ multiplied with the terminal falling velocity $v(D)$. From this product the rain rate is obtained by integration over the drop size

$$RR = \frac{\pi}{6} \int_0^\infty N(D)D^3 V(D)dD \quad (2)$$

1.4. Radar Reflectivity

The Rayleigh approximation, which takes into account the scattering of rain molecules less than the wavelength of the emitted microwave, and produces a signal of equal power, is used to calculate the radar reflectivity factor of an amount of liquid and spherical particles. This factor is stated in mm^6/m^3 . It is independent of the radar frequency's wavelength. In addition, the sixth instant of the rain drop size distribution is the radar reflectivity. So, it is possible to compare the measurements made by several radars operating at various frequencies. Consequently, it can be written as

$$Z = \int_0^\infty N(D)D^6 dD \quad (3)$$

and in logarithmic form it is expressed as:

$$dBZ = 10 \log_{10} \frac{Z}{Z_{ref}} \quad (4)$$

where $Z_{ref} = 1 \text{ mm}^6 / m^3$

1.5. Liquid Water Content (LWC or M)

The quantity of liquid water in a given mass of dry air is known as the liquid water content (LWC). It is commonly measured in grams per cubic meter (g/m^3) of air or grams per kilogram (g/kg) of air.

It is the result of dividing the scattering volume by the sum of the volumes of all the droplets with the water density w . Therefore, it relates to the drop size distribution's third moment

$$LWC = \rho_w \frac{\pi}{6} \int_0^{\infty} N(D) D^3 dD \quad (5)$$

Based on the kind of clouds that are present in the sky at a particular place, a cloud's liquid water content might vary greatly.

1.6. Fall Velocity

An adequate definition of the drop velocity that contributes the most to the total rate of precipitation. Wind profilers employ the first moment of the Doppler spectra, also known as the spectra volume density, to determine the radial velocities. Since the falling velocity is determined by the drop size for each one of the drops, it is also straightforward to find using the distribution of drop sizes. The equilibrium between the forces of gravity and air drag that control a raindrop's descent will be attained when the raindrop reaches its terminal velocity in the calm atmosphere. Under these circumstances, it is possible in theory to calculate the terminal velocity in line with this expression from [4].

$$V^2 = \frac{4}{3} g d (\rho_s - \rho) / \rho c \quad (6)$$

Where V is the terminal velocity of fall, ρ and ρ_s are respectively the air and raindrop densities, μ is atmospheric drag coefficient, g is gravity acceleration, c is the drag coefficient and d is the diameter of the raindrop.

1.7. Principle of Operation of Weather Radar

Sending Radar Pulses

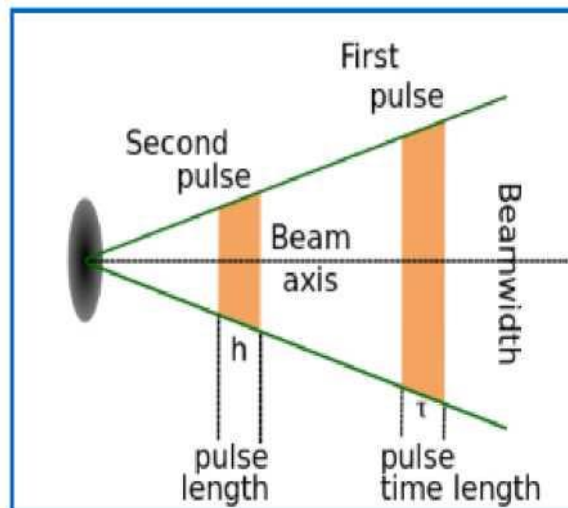


Figure 1: A radar beam spreads out as it moves away from the radar station, covering an increasingly large volume.

Weather radars send directional pulses of microwave radiation, on the order of a microsecond long, using a cavity magnetron or klystron tube connected by a waveguide to a parabolic antenna. The wavelengths of 1 - 10 cm are approximately ten times the diameter of the droplets or ice particles of interest, because Rayleigh scattering occurs at these frequencies. This means that part of the energy of each pulse will bounce off these small particles, back in the direction of the radar station [11].

Shorter wavelengths are useful for smaller particles, but the signal is more quickly attenuated. Thus 10 cm (S-band) radar is preferred but is more expensive than a 5 cm C-band system.

3 cm X-band radar is used only for short-range units, and 1 cm Ka-band weather radar is used only for research on small-particle phenomena such as drizzle and fog W band weather radar systems have seen limited university use, but due to quicker attenuation, most data are not operational.

Radar pulses spread out as they move away from the radar station. Thus the volume of air that a radar pulse is traversing is larger for areas farther away from the station, and smaller for nearby areas, decreasing resolution at far distances. At the end of a 150 - 200 km sounding range, the volume of air scanned by a single pulse might be on the order of a cubic kilometer. The volume of air that a given pulse takes up at any point in time may be approximated by the formula

$$v = hr^2$$

where v is the volume enclosed by the pulse, h is pulse width (in e.g. meters, calculated from the duration in seconds of the pulse times the speed of light), r is the distance from the radar that the

pulse has already travelled (in e.g. meters), and is the beam width (in radians). This formula assumes the beam is symmetrically circular, " r " is much greater than " h " so " r " taken at the beginning or at the end of the pulse is almost the same, and the shape of the volume is a cone frustum of depth " h ".

1.8. Project Site

The Federal University of Technology in Akure, Ondo State, Nigeria (7°15'N, 5°15'E) was chosen as the study's measuring location.

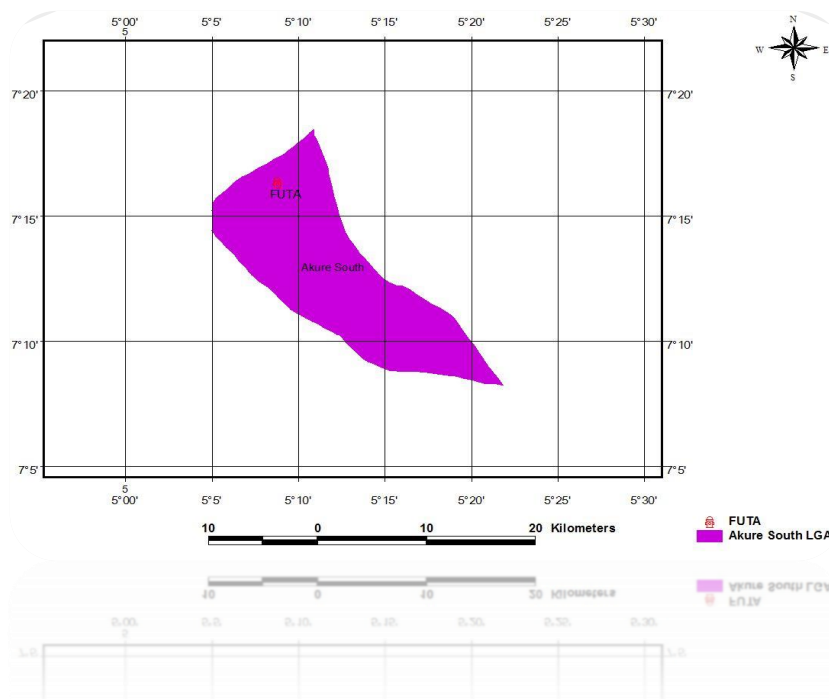


Figure 2: Map of measuring site

This experiment was conducted in Ondo State, South-Western Nigeria, which is made up of lowlands and rough hills with granitic outcrops in a few locations. Generally speaking, the land slopes from the southern coastal region (less than 15 meters above sea level) to the rocky hills

of the northern section. Ondo State has a Lowland Tropical Rain Forest climate, which features different dry and wet seasons. The average monthly temperature in the south is around 27°C, with an average monthly range of 2°C, and the average relative humidity is over 75%. However, the average monthly temperature and its range in the northern section of the country are roughly 30°C and 6°C, correspondingly. The mean monthly relative humidity is less than seventy per cent. In the south, rain rains every day of the year with the possible exception of November, December, and January, which can be comparatively dry. The average yearly total precipitation is more than 2000 millimeters. The North, however, experiences a distinct dry season from November to March during which little to no rain occurs. As a result, the annual rainfall total in the north is much lower, at roughly 1800 millimeters.

2. Methodology

The Micro Rain Radar's measuring methodology is based on electromagnetic waves with a frequency of 24 GHz. The signals are transmitted vertically into the atmosphere as opposed to horizontally like standard rain radar equipment. Raindrops deflect some of the transmitted signal back to the parabolic antenna. As opposed to pulsed radars, the output signal is sent continuously (CW mode). The Micro Rain Radar is a Doppler radar, which means that as raindrops hit the ground, they move relative to the ground-based antenna, which serves as both a transmitter and a receiver.

Utilizing the threshold rain rates of $R \leq 10$ mm/h for stratiform rain and $R > 10$ mm/h for convective rain events [12], the data were further classified into stratiform and convective rainfall. As Convective precipitation areas are typically characterized by sporadic great vertical velocities, high rain rates (>5 mm/hr), and small intense cells (1-10 km in horizontal dimension). According to [13], stratiform precipitation zones are distinguished by modest rainfall rates (5 mm/hr) and small vertical velocities (100-km horizontal dimension). Due to their stratiform character, the rainfall events on July 11 and July 3 were stratiform in nature and on July 10 was convective due to their high rain rate.

The sent and received signals differ in frequency by a quantity known as Doppler frequency because of how quickly raindrops fall in relation to a fixed antenna. This frequency serves as a gauge for the raindrops' rate of descent. According to [10], different raindrop diameters have varied falling velocities, hence the backscattered signal is made up of a distribution of various Doppler frequencies. This signal's spectral analysis produces a large spread of lines that correspond to the signal's Doppler frequencies. The drop spectrum is computed from the Doppler spectrum while taking into account the transfer function of the radar module by the radar electronics, which calculates this spectrum with a high time resolution of 10 seconds. The real rain rate and the liquid water content are obtained by integrating over the whole drop spectrum, taking additional correction factors into account, and then averaging for 30 seconds. The Doppler spectrum is measured by the Micro Rain Radar between 0 and 12 m/s. The connection provided by [10] is used in the typical real-time processing to relate drop sizes to Doppler velocities. The rain drop numbers are then determined from the spectral volume reflectivity using the Mie theory. Corrections are made for irregular raindrops and lower air densities that result in faster falling velocities at high elevations. Calculating Mie extinction from the given DSD results in the proper attenuation correction for moderately elevated rain rates. While the average falling velocity (first Doppler moment) and integral reflectivity (zeroth Doppler moment) are computed directly from the recorded Doppler spectrum, the rain rate, liquid water content (LWC), and Rayleigh reflectivity Z are estimated from the DSD. The range

resolution of the Micro Rain Radar can be adjusted from 10 to 200 m in 30 height intervals. The usage of ranges greater than 6 km is prohibited by attenuation at 24 GHz.

3. Results and Discussion

After being gathered from the raw data collected as shown in Figures 3 to 8, the variations of the rain rate and liquid water content with height was assessed for the one week of data. These demonstrate that in all cases taken into account, the highest rain rate and liquid water content were noted along elevations of 2000–30000 m. The consequence of this is that, in comparison to other height bins, we should anticipate increased radio wave attenuation along this height. This is so since at this height, compared to greater height levels, wind and hydrodynamic forces are less intense. Figures 3–8 additionally illustrate the relationship between rain rate and liquid water content in respect to height and the correlation between these two variables across all rain categories.

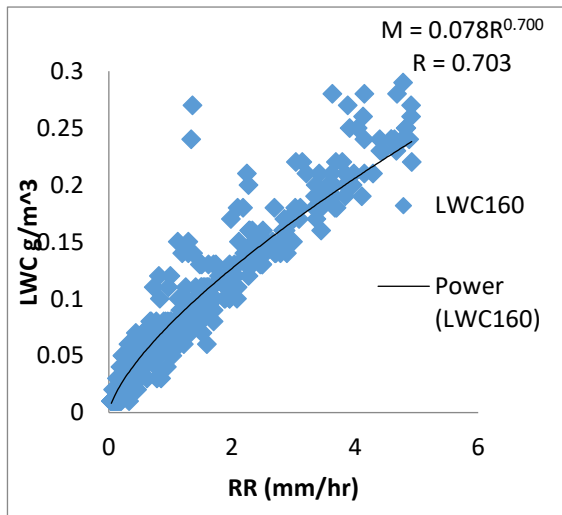


Fig 3: M-R relation at height 160m for Drizzle (2014)

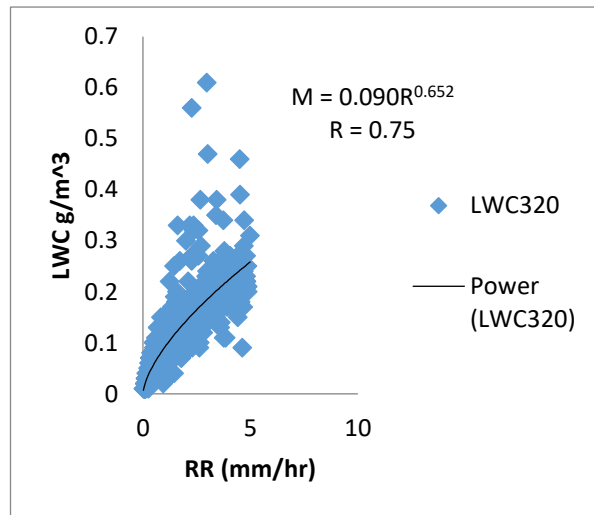


Fig 4: M-R relation at height 320m for Drizzle (2014)

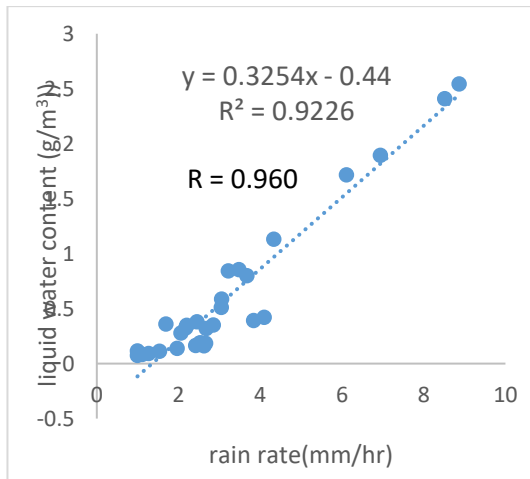


Figure 5: Variation of Average Liquid water content with average

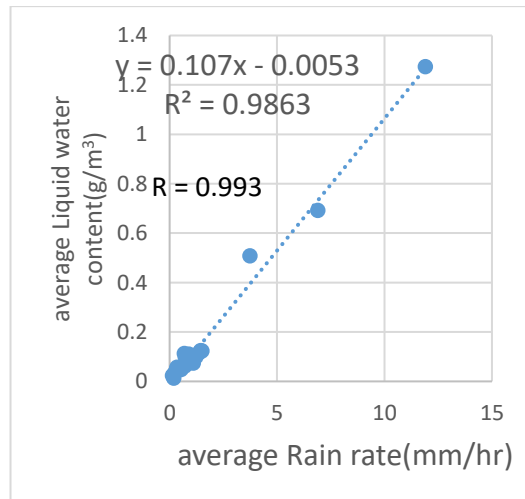


Figure 6: Average Liquid water content (g/m3) against average Rain rate (mm/hr) Rain rate .height for August 2014.

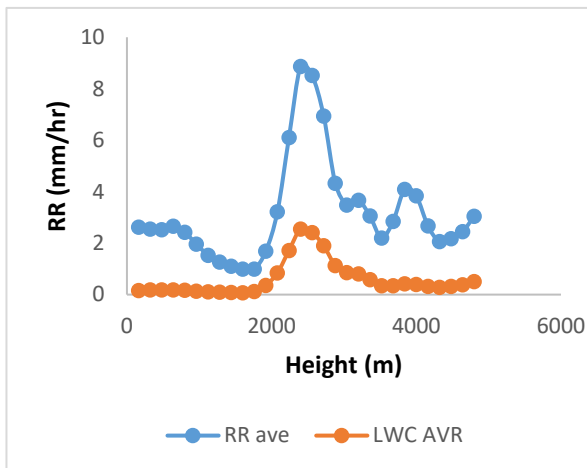


Figure 7: Variation of Average rain rate with heights for July 2009

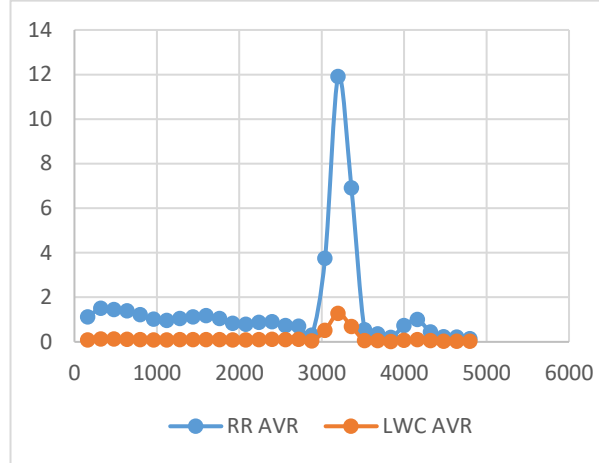


Figure 8: Average RR(mm/hr) and average LWC(g/m³) against height(m)

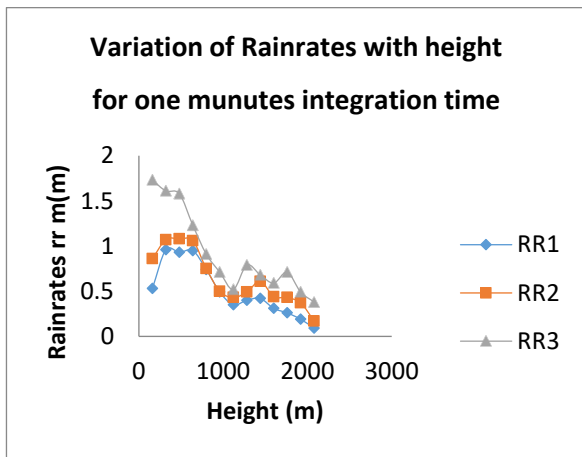


Figure 9: Variation of Average Rain rate with height for minute integration time for September 2014

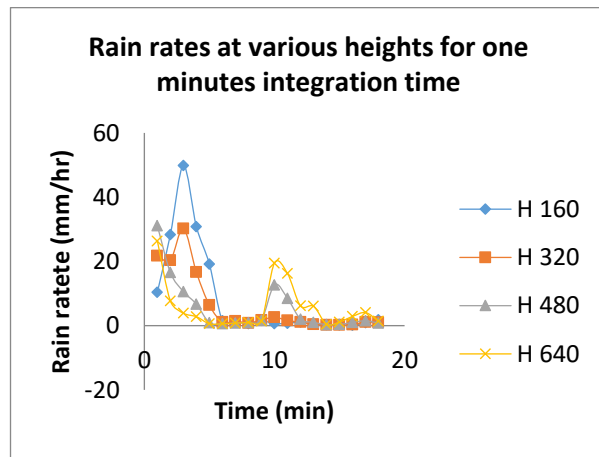


Figure 10: Variation of Rain rates at various heights for one min one integration time for September 2014

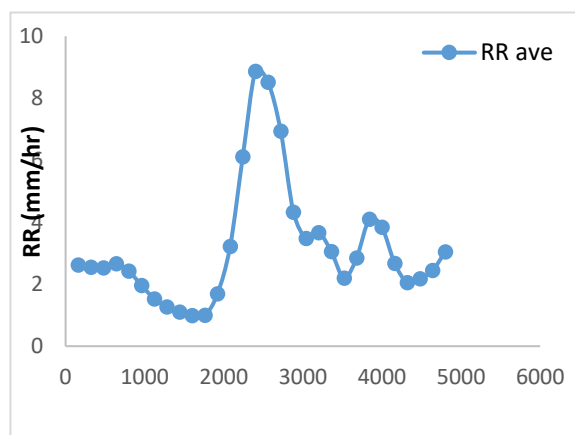


Figure 11: Variation of Average Rain rate with height for Aug 2014

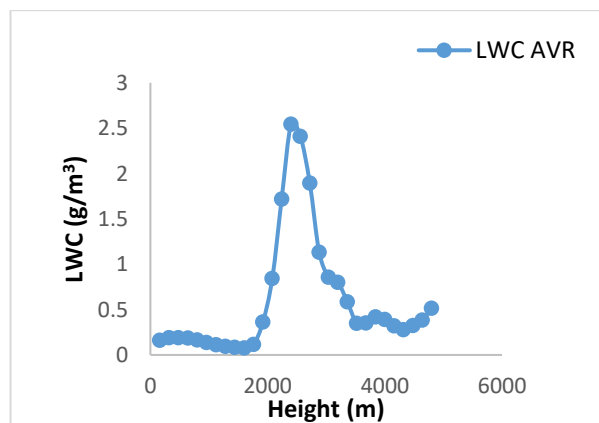


Figure 12: Variation of Average Liquid water content with height for Aug 2014

3.1. Rain rate or rain attenuation time series using MRR at different heights

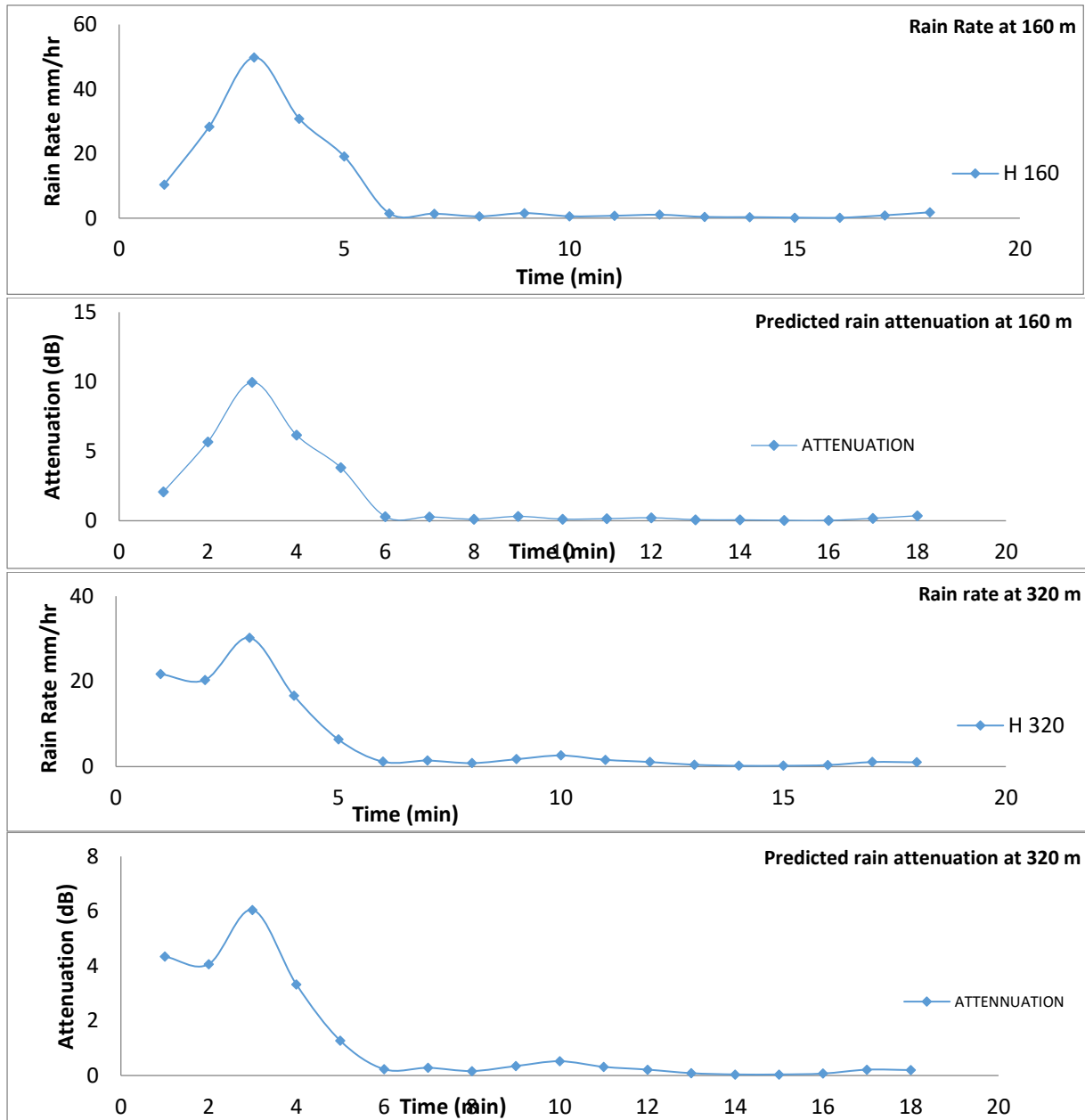


Figure 13: Rain rate or rain attenuation time series converted by SST for measured rainy events

3.2. Results Analysis

Figures 3 to 6 are plots from the power law relation from the data obtained for the year during the particular rain events. Drizzle rain events (i. e. for rain rates ≤ 5 mm/hr) was considered here at heights 160 m and 320 m. Here a good correlation was observed as shown from the power law fit from the scattered plot. The power law coefficient a and exponent b for heights 160 m are given as 0.078 and 0.7 with correlation coefficient of 0.7. Also, for height 320 m, the power law coefficient a and the exponent b are given as 0.09 and 0.652 with correlation coefficient 0.75. Results obtained were compared with those obtained at some other tropical locations as shown in the work of [13]. Values of correlation coefficient were over 70 % for all cases indicating a relatively high degree of correlation for LWC and RR.

The scatter graphs (Figure 5 and 6) above show the regression line, correlation coefficient, and liquid water content for the varied daily mean precipitation for the year 2014. In all cases taken into account, there is a significant degree of connection; for the majority of rain kinds, the coefficients of correlation are better than 0.91. For each type of rain, equivalent power relationships were found. For a tropical station, Akure in Nigeria, the rainfall metrics collected for the one week under consideration have been examined.

Figures 7 to 12 shows the variations of average rain rates, Liquid water content with heights for the year under review and it was noted that the rain rate between 0 and 10 mm/hr (stratiform rain) from the heights of 0 – 4800 m above sea level contributed the most to the rain event. As a result, stratiform rainfall was reported during two days in August and September 2014 of meticulous observation and data collection, with the maximum rain rate recorded in the height range 2400 to 3200 m. Using least square power law regression, empirical relationships between rainfall rate and liquid water content for different forms of rain have been found. The stratiform rain fall rate $R < 10 \text{ mm/h}$ and convective rain rate $R > 10 \text{ mm/h}$ criteria from [12] were used to categorize the measured rainfall rates.

In years 2014, all rain events were observed and the results are as shown above. Since rain attenuation can be expressed as a function of rain rate, the contribution of an individual drops to impaired radio signals can also be predicted. All the rain events In August 2021 at different heights was observed and recorded with the results shown in Figure 13. Using equation 10 all the rain events were converted to rain attenuation time series for heights 160 and 320 m and the plots obtained are as shown. The plots demonstrate strong correlation throughout the event. The predicted rain attenuation time series also follows similar pattern observed in rain rate time series for the different heights under consideration. The attenuation is at its peak of 9.96 dB when the rain rate is 49.82 mm/hr for height 160 m above sea level. Similarly for height 320 m, the attenuation is at its peak with the value of 6.05 dB when the rain rate is 30.25 mm/hr. The difference explains why the effect of attenuation of radio signals are mostly felt at the ground level than at higher altitudes.

4. Conclusion

Using the conditions of [14], the observed rainfall rates were divided into two groups, namely for stratiform rain rate, $R < 10 \text{ mm/h}$, and for convective rain rate, $R \geq 10 \text{ mm/h}$, in order to assess the variation of rainfall parameters with height using Micro Rain Radar. Figure 4-12 depicts the rate of precipitation and the liquid water content at various altitudes. It is clear that stratiform rain predominated the event, lasting a longer time and falling primarily at night.

The results depict the rate of precipitation and the liquid water content as a function of height. Convective cells only generated rain rates considerably above 10 mm/hr for a brief period for each form of rainfall, as can be shown. Examples are shown in figures 9 and 11 at elevations of 3200 m. For the different days and height ranges considered, the stratiform and convective rainfall rate, liquid water content, and height relationships have been found to have good correlation coefficients and graphs (0.92), and the convective rainfall type also has an outstanding correlation coefficient (> 0.85). The difference in the time series of the rain attenuation so obtained explains why the effect of radio signals are mostly felt at the ground level than at higher altitudes.

Reference

- [1] Harikumar (2009), "Study of tropical rain drop size distribution and integral rain parameters using ground based and satellite measurements", phd Thesis.
- [2] Shengjie N., Xingcan J., Jianren S., Xiaoli L., Chunsong L., and Yangang L., "Distributions of Raindrop Sizes and Fall Velocities in a Semiarid Plateau Climate: Convective versus Stratiform Rains", Journal of Applied Meteorology and Climatology, vol. 49, pp. 632-645.
- [3] Rogers R. R., I. I. Zawadzki and E. E. Gossard (1991): "Variation with altitude of the drop-size distribution in steady light rain", quart Journal Roy Meteor Society, vol. 117, pg 1341-1369.
- [4] Gunn, R., and Kinzer, G. D. (1949): "The terminal velocity of fall for water drops in stagnant air". Journal of Meteorology, vol. 6, pp 243-248.
- [5] Guillermo Montero-Martez, Alexander B., Kostinski, Raymond A Shaw and Fernando Garcia-Garcia (2009), "Do all rain drop at terminal speed?", Geophysical Research Letters, vol. 36 L11818, pp. 1-4
- [6] Diederich M., S. Crewell, C. Simmer and R. Uijlenhoet (2004), "Investigation of rainfall microstructure and variability using a vertically pointing radar and disdrometer", ERAD proceedings, pp. 80-86
- [7] METEK "Meteorologische Messtechnik, gmbh (2005)", Micro Rain Radar Physical Basics, Version 1.8.3.
- [8] Narayana T. Rao, N. V. P. Kirankumar, B. Radhakrishna and D. Narayana Rao (2007), "Classification of tropical precipitating systems using wind profiler spectra moments". Journal of Atmospheric and oceanic Technology", Vol. 25, pp. 884-897.
- [9] Ajewole M.O, Kolawole L.B and Ajayi, G.O (1999): "Theoretical study of the effect of different types of Tropical rainfall on microwave and millimeter-wave Propagation". Journal of Radio Science, vol34, No 5, pg 1103-1124
- [10] Atlas D., R. C. Srivastava and R. S. Sekhon (1973): "Doppler radar characteristics of precipitation at vertical incidence", Reviews of Geophysics and Space Physics. Vol. II pg 1.
- [11] Doviak R. J and Zrnicek R. S. (1993), "Radar and its Environment", 2nd Edition Doppler Radar and Weather observations, pp. 30 – 63.
- [12] Maheh Konwar, Diganta Kumar Sarma, Jyotirmoy Das & Sanjay Shama (2006), "Shape of the rain drop size distributions and classification of rain type at Gadanki", Indian Journal of Radio and space Physics. Vol. 35, pp. 360-367.
- [13] Joss J. And A. Waldvogel (1968): "Raindrop size distribution and sampling size errors", Journal of Atmospheric Science, vol. 26, pg 566-569
- [14] Izeukou, A., Sauvageot, A., Ochou D., and Kebe, C. M. F. (2004): "Raindrop size distribution and radar parameters at Cape Verde", Journal of Applied Meteorology, vol. 43, pp. 90-105.